DYNAMIC RESPONSE OF AXONAL MICROTUBULES UNDER SUDDENLY APPLIED END FORCES

Farid Manuchehrfar, Amir Shamloo and Nastaran Mehboudi

Abstract— **Axon is a filament in neuronal system and axonal microtubules are bundles in axons. In axons, microtubules are coated with microtubule-associated protein tau, a natively unfolded profuse filamentous protein in the central nervous system. These proteins are responsible for the cross-linked structure of the axonal microtubule bundles. Through complimentary dimerization with other tau proteins, bridges are formed to nearby microtubules to create bundles. The transverse reinforcement of microtubules by cross-linking to the cytoskeleton has been shown to enhance their ability to bear compressive loads. Though microtubules are conventionally regarded as bearing compressive loads, in certain circumstances such as in traumatic stretch injury, they are placed in tension. We employ Standard Linear Solid, a viscoelastic model, to computationally simulate microtubules. This study investigates the dynamic response of two dimensional axonal microtubules under suddenly applied end forces. We obtain the results for steady state behavior of axonal microtubule for different forces.**

I. Introduction

Axon is one of the most important parts of the neuronal cells and axonal microtubules are fibers in axons (Fig. 1). The main function of microtubules is stabilizing the neuronal axons. Microtubule bundles located in the inner part of the axons have polar orientation [1]. Microtubules have cross linked with tau proteins. These tau proteins are the main factor of axonal strength and cause some electrical pulse to be emitted out of neurons (Fig. 1).

There are several models for action of microtubules, axons or neurons. In fact, microtubules are the main parts of axons that protect them from mechanical strain. Size of microtubules and spatial position of these bundles in microtubules are discussed in 1980s and 1990s [1]. Tau proteins connect microtubules transversally. Geometry of these bundles are formed by their cross links.

The injuries of microtubules are the main cause of stroke that happens during damage of axons or retraction of synapses [4] [2]. Microtubules are shown to rapture under the strain of about 50% [3].

In 2010, a mathematical model was studied the dynamics of microtubules [5]. In this model, microtubular bundles were assumed to be discrete masses. They pose linear springs between masses but the stiffness of microtubules was not linear and they behaved such as a viscoelastic material. This has been observed in all experiments performed on axons.

One of the models for axons in the recent years was suggested by [4]. They endeavored to model the axon under tension. In this model microtubules were assumed to be in hexagonal positions and each microtubule bundle was considered to have a discontinuity. There are 19 microtubule bundles in each axon.

Microtubule bundles have been recently studied widely. One of the recent studies has used finite element method to model axons under tension and torsion [6].

Our main goal is to receive an appropriate model of axonal microtubules. In this model the dynamic response of microtubule bundle under the action of suddenly applied end forces was studied. Microtubules were connected to their neighboring microtubules using tau proteins that were the main feature providing axonal stiffness. As it is shown in Fig. 1, an axon is a part of the neuronal cell and axonal microtubules are located in the interior part of the axons.

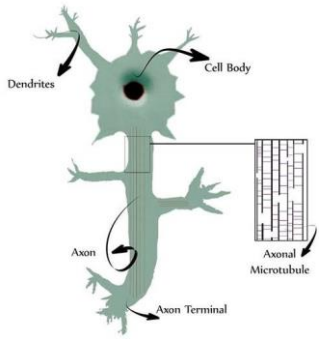

Fig. 1 Schematic of a Neuron with an Axon, Dendrites, Axonal terminals and Microtubules.

II. Methods

A. Viscoelasticity

Mechanical modeling of materials can be easier by springs and dampers. Springs show the behavior of hookian solids and dampers remark the behavior of Newtonian fluids. A viscoelastic material behaves as a mixture of springs and dampers. We can model viscoelastic materials by using the combination of springs and dampers in series and parallel. For example *Maxwell* and *Kelvin-Voigt* models are the two introduced models for viscoelastic materials. As depicted in Fig. 2, Kelvin-Voigt model is represented by a spring and a damper in parallel and Maxwell model consists of a spring

F.Manuchehrfar is with the Sharif University of Technology, Tehran, Iran,

A.Shamloo is with the Department of Mechanical Engineering, Sharif University of Technology, Tehran, Iran, (e-mail: shamloo@sharif.edu).

N. Mehboudi is with the Department of Mechanical Engineering, Sharif University of Technology, Tehran, Iran

978-1-4244-7929-0/14/$26.00 ©2014 IEEE

and damper in series.

Maxwell and Kelvin-Voigt models have some limitations in which they do not model viscoelastic materials for all possible conditions. Kelvin-Voigt model does not predict relaxation and Maxwell model is insufficient for creep test. *Standard Linear Solid (SLS)* is a combination of Maxwell and Kelvin-Voigt models. This model is a simple model which predicts creep and relaxation simultaneously. The three aforementioned viscoelastic models are schematically represented in Fig. 2.

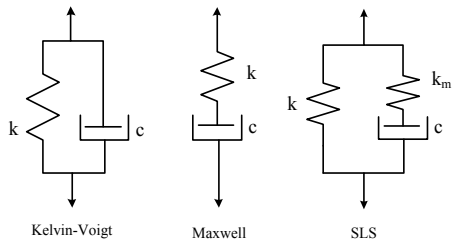

Fig. 2 Schematic of 3 major viscoelastic models

As depicted in Fig. 2, SLS model consists of a spring which is in parallel with a series of dashpot-spring pair. The right arm consists of a spring, k_m and a damper, c. This arm is typically called Maxwell arm. The left arm is simply a linear spring, k.

Consider the system depicted in Fig. 2, in which a discrete point mass is linked to a stationary wall through a SLS unit. In what follows, it is considered that the mass is acted upon by a given force F(t) and the governing equations for its motion are tackled with. The governing equations can be written as follows

$$M\ddot{x} = F - kx - c(\dot{x} - \dot{x}_m) \quad (1)$$

$$c(\dot{x} - \dot{x}_m) - k_m x_m = 0 \quad (2)$$

In order to gain some insight into the behavior of this model in response to a given input force, a step-like constant force can be considered that is imposed on the stationary mass at the initial time. The governing equations for this case are simplified in (3) & (4).

$$\ddot{x} = f_0 - \omega^2 x - 2\eta\omega(\dot{x} - \dot{x}_m) \quad (3)$$

$$\dot{x} - \dot{x}_m - \frac{\omega_m^2}{2\eta\omega} x_m = 0 \quad (4)$$

where, $\omega = \sqrt{k/M}$, $\omega_m = \sqrt{k_m/M}$, and $\eta = c/2\sqrt{Mk}$.

B. Numerical Method

Since the analytical solution of this system of ordinary differential equations is a bit laborious, numerical integration is utilized in order to find the resulting response. In order to tackle with the problem numerically, Velocity Verlet integration methodology is one of the most commonly used algorithms. This is efficiently used to numerically integrate the Newton's second law of motion. Given the position, velocity and acceleration of a point mass at a specific instance of time, the velocity and position after a short time interval, Δt , are determined.

C. Forces

For the sake of generality, the initial spacing between the microtubules is considered to be χ times the initial spacing between two adjacent point masses in a given microtubule. The stiffness and damping coefficient of the tranverse links are assumed to be respectively φ and ψ times of their counterparts in microtubular links. The system is assumed to be initially all at rest.

The governing equations of motion for the two coordinates can be formulated as given in (5)-(6)

$$\ddot{x}_i^{\bullet} = \sum_p f_{pi,x}^{\bullet} - \sum_j a_d(a + b\varphi + c\kappa)\left(x_i^{\bullet} - x_j^{\bullet} - (a + b\chi + c/2)\alpha_{ji}\right) - 2\xi \sum_j a_d(d + b\psi)\left[(\dot{x}_i^{\bullet} - \dot{x}_j^{\bullet})\alpha_{ji}^2 + (\dot{y}_i^{\bullet} - \dot{y}_j^{\bullet})\alpha_{ji}\beta_{ji}\right] + \ddot{x}_{Bending}^{\bullet} \quad (5)$$

$$\ddot{y}_i^{\bullet} = \sum_p f_{pi,y}^{\bullet} - \sum_j a_d(a + b\varphi + c\kappa)\left(y_i^{\bullet} - y_j^{\bullet} - (a + b\chi + c/2)\beta_{ji}\right) - 2\xi \sum_j a_d(d + b\psi)\left[(\dot{x}_i^{\bullet} - \dot{x}_j^{\bullet})\alpha_{ji}\beta_{ji} + (\dot{y}_i^{\bullet} - \dot{y}_j^{\bullet})\beta_{ji}^2\right] - 2\xi' \dot{y}_i^{\bullet} + \ddot{y}_{Bending}^{\bullet} \quad (6)$$

The governing equations have 5 main parts. The first right-hand side summation is over all the possible external forces acting on point masses indexed by *i*. The second and third summations are over elastic and dissipative forces affecting a point mass indexed by *i* through its links to other neighboring point masses or nodal points, where the serial damper and spring meet. In these equations *a*, *b*, *c*, and *d* are indicators of whether the neighborhood is one between two point masses in the same microtubule via a linear spring; between two transverse point masses via cross-linking proteins and a parallel damper; between a point mass and a nodal point through a spring; between a point mass and a node through a dissipative element. These indicators assume only binary values of unity and zero with respect to whether the respective neighborhood exists or doesn't hold. More specifically, if *a* is set to unity and the others are set to zero, the neighborhood is the one between two point masses in the same microtubule through a linear spring. The first constant under the summations, a_d, is called discontinuity indicator which also assumes values of unity or zero and indicates whether the neighborhood fades as a result of any possible discontinuity. α_{ji} and β_{ji} also represent the *x* and *y* components of unit vector directed from point mass *j* to point mass or node *i*. In these equations ζ' is the damping ratio of the motion in the normal direction of the applied forces.

The last term in the governing equations refers to bending acceleration. In order to formulate the bending moment, three given point masses can be considered as depicted in Fig. 3. At any instance of time a plane can be constructed for each trio of neighboring points. The normal vector of this plane is calculated from Table 1. $\hat{n}_{i,i+1}$ and $\hat{n}_{i,i-1}$ are unit normal vectors pointing from mass *i* toward masses *i + 1* and *i - 1*. 'ξ' and 'η' are components of $\vec{r}_{i,i+1}$ in the direction and normal to the $\vec{r}_{i,i-1}$. Angular deformation, α is measured with respect to 'ξ' and 'η' as can be seen in Table

1. In order to calculate 'ξ' and 'η', first we calculate the unit normal vector $\hat{m}$ which stands normal to the $\vec{r}_{i,i-1}$ in the plane of three point masses. After the calculation of the angular deformation, the restoring moment and accelerations can be determined. Table 1 shows the calculation of bending acceleration and describes the parameters that are needed.

TABLE I. CALCULATION OF BENDING ACCELERATION

Parameter	Description	Calculation or Source
$\vec{r}_{i,i-1}$	Position of mass i-1 related to mass i	-
$\hat{n}_{i,i-1}$	Unit vector of $\vec{r}_{i,i-1}$	-
$\vec{r}_{i,i+1}$	Position of mass i+1 related to mass i	-
$\hat{n}_{i,i+1}$	Unit vector of $\vec{r}_{i,i+1}$	-
$\hat{n}$	Normal vector to $\hat{n}_{i,i+1}$ and $\hat{n}_{i,i-1}$	$\hat{n} = \frac{\hat{n}_{i,i+1} \times \hat{n}_{i,i-1}}{\lvert \hat{n}_{i,i+1} \times \hat{n}_{i,i-1} \rvert}$
$\hat{m}$	Normal vector to $\vec{r}_{i,i-1}$ in the plane of 3 point masses	$\hat{m} = \hat{n}_{i,i-1} \times \hat{n}$
ξ	Component of $\vec{r}_{i,i+1}$ in the direction of $\vec{r}_{i,i-1}$	$\xi = -\hat{n}_{i,i+1}\hat{n}_{i,i-1}$
η	Component of $\vec{r}_{i,i+1}$ in the direction of $\hat{m}$	$\eta = \hat{n}_{i,i+1} \cdot \hat{m}$
α	Angular deformation	$\alpha = tan^{-1}(\frac{\eta}{\xi})$
T	Torsion on point masses i-1 and i+1	$\vec{T} = k_b \alpha \hat{n}$
k_b	Bending stiffness	Stephan et al. [4]
$\ddot{\vec{r}}_{i,i-1}$	Acceleration of point mass i-1 cause by point mass i	$\ddot{r}_{b,i-1} = \ddot{r}_{b,i} + \frac{\vec{T} \times \vec{r}_{i,i-1}}{m_{i-1} r_{i,i-1}^2}$
$\ddot{\vec{r}}_{i,i+1}$	Acceleration of point mass i+1 cause by point mass i	$\ddot{r}_{b,i+1} = \ddot{r}_{b,i} + \frac{\vec{T} \times \vec{r}_{i,i+1}}{m_{i+1} r_{i,i+1}^2}$

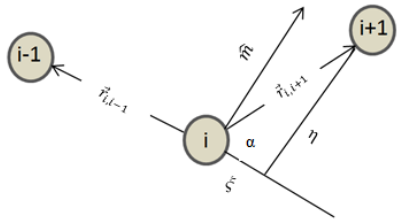

Fig. 3 Representation of three discrete masses connected together

III. GEOMETRY

The simplified microtubular geometry proposed in [4] consists of a hexagonal array of 19 rows. The cross-sectional view of three dimensional geometry reconstructed on our computational platform is presented in Fig. 4(a). Since at this stage, we tend to work with non-dimensional equations, the characteristic length scale is assumed to be the distance between two neighboring points in a bundle. According to [4] the microtubular spacing should be 4.5. In Fig. 4(a) dashed lines represents tau proteins and jots indicate the microtubule bundles. This Figure is in z-y plane.

We modeled microtubule bundles in 2 dimensional frames. Each microtubule bundle has one point of discontinuity. The point of discontinuity is designated on a random basis and is assumed to be within the central 80% of the geometry length. According to the dimensions presented by [4] each row is an ensemble of 800 point masses. We have used a variety of number of point masses from 80 to 800 and we assumed number of microtubules to be eight. A bird's-eye view of the entire geometry is given in Fig. 4(b). The dashed lines represent cross-links attributed to tau proteins and blue lines show microtubule bundles in x-y plane.

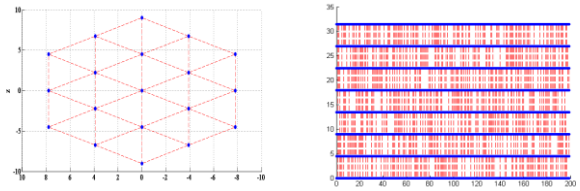

(a) (b)

Fig. 4 (a) The cross-sectional view of a three dimensional geometry and (b) a view of the entire geometry

IV. RESULTS AND CONCLUSION

Material parameters were prepared from [4]. Now if the system depicted in Fig. 4(b), is acted upon on both sides by constant external forces affecting opposite to each other, it embarks on a time-varying deformation. The overall deformation of the system is defined as (7). The first and second summations are over the rightmost and leftmost points. 'n' and 'L^*' are the number of microtubules and the initial length of the system.

$$Strain = \frac{\sum x_{i,r}^* - \sum x_{i,1}^*}{nL^*} \tag{7}$$

The time-step should be not too large that the results are prone to considerable error, and not too small that the computation cost increases. Before starting the solution we try to cast equations into a non-dimensional form. The non-dimensional variables are defined in (8) that $t_0 = \sqrt{\frac{M}{K}}$, x_0 is the distance between each two neighboring masses in a bundle and $f_0 = Kx_0$ is a characteristic value for the force imposed upon the system. Introducing these new variables gives rise to the non-dimensional equations of motion given in (9) and (10), where $\kappa = k_m/k$ is itself a non-dimensional parameter.

$$t^* = \frac{t}{t_0} \qquad x^* = \frac{x}{x_0} \qquad F^* = \frac{F}{F_0} \tag{8}$$

$$\frac{d^2x^*}{dt^{*2}} + 2\eta\left\{\frac{dx^*}{dt^*} - \frac{dx_m^*}{dt^*}\right\} + x^* = F^* \tag{9}$$

$$2\eta\left\{\frac{dx^*}{dt^*} - \frac{dx^*{}_m}{dt^*}\right\} + \kappa x_m^* = 0 \tag{10}$$

Using system with a SLS unit with 1 mass we found that appropriate value for time step is 0.0025. We modeled the fluid around the microtubules with a damper connected to each point mass that dissipates the energy of microtubules in x and y directions. The value of non-dimensional damping ratio is assumed to be 1.

We solved the system for discrete mass numbers of 100, 400 and 800 and the non-dimensional forces values of 0.1, 0.75, 1 & 4. Fig.5 illustrates the dynamic response of 2D microtubule bundles consisted of 400 masses under different forces.

Using information in fig. 5 we can assume that the steady state strain is the fourth degree polynomial function of non-

dimensional force. So we can write an equation for the steady state strain and draw the steady state strain as a function of applied force as depicted in fig. 6.

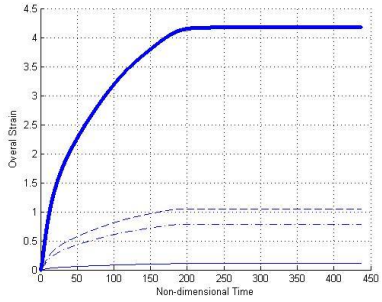

Fig. 5 Bundle Dynamic for 400 discrete masses for F^*=0.1 (solid line), F^*=0.75 (dotted line), F^*=1 (dashed line) and F^*=4 (solid thick line)

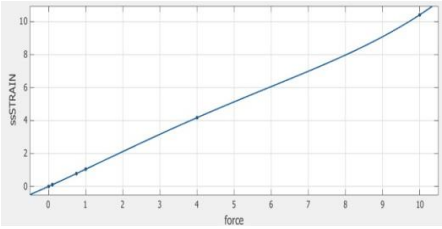

$$ssSTRAIN = 7.88 \times 10^{-4} F^{*4} - 0.0117 F^{*3} + 0.041 F^{*2} + 1.016 F^{*1} + 0.0028$$

Fig. 6 Steady State Strain as a function of force

If we decrease the number of single masses per microtubule bundles, discontinuities play more important role and dissipation becomes more prominent as it is pointed in Fig 7. Fig. 7 is prepared for f^*=0.1 and compere microtubule dynamic response for discrete masses of 100 and 400.

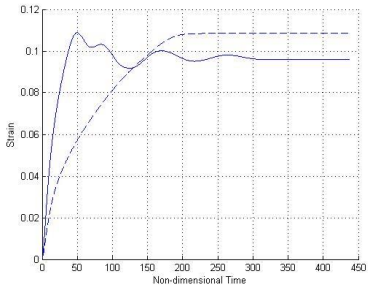

Fig 7 Strain-Time diagram for the number of single mass per microtubule=100 (solid line) and 400(dashed line)

In this step we check a two dimensional system of microtubule with 800 discrete masses per microtubule. We prepared Fig. 8 for different quantities of non-dimensional forces. Fig. 9 shows steady state behavior of a 2D axonal microtubule as a forth degree polynomial function of non-dimensional applied force.

As it is specified from Fig. 8, Fig. 7 and fig. 5, when we increase the number of discrete masses, the needed time to reach steady state growth. We are extending our model to simulate the rupture of axons under tension that is one of the main causes of stroke.

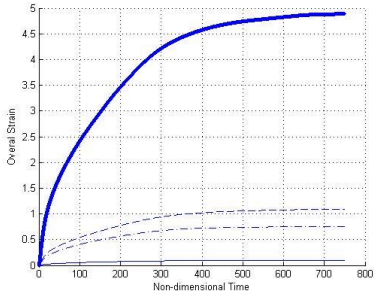

Fig. 8 Bundle dynamics for 800 discrete masses for F^*=0.1 (solid line), F^*=0.75 (dotted line), F^*=1 (dashed line) and F^*=4 (solid thick line)

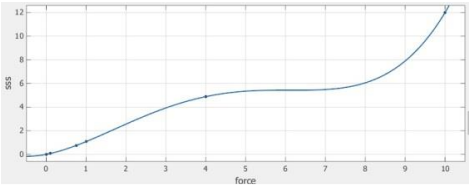

$$ssSTRAIN = 8.88 \times 10^{-3} F^{*4} - 0.138 F^{*3} + 0.552 F^{*2} + 0.655 F^{*1} + 0.0083$$

Fig. 9 Steady State Strain as a function of force

We received an appropriate model to compute the behavior of 2 dimensional axonal microtubules under suddenly applied end forces without accounting the effect of axonal rapture. To improve our model we will add this effect to our model. We also assumed the fluid around the microtubule bundles as dissipative elements with constant damping ratio of 1. We will calculate the exact behavior of the fluid around to receive an equation or constant value for damping ratio using an exact model in the future.

REFERENCES

[1] Fadic, R., J. Vergara, and J. Alvarez. 1985. Microtubules and caliber of central and peripheral processes of sensory axons. J. Comp. Neurol. 236:258–264.

[2] Tang-Schomer, M. D., A. R. Patel, D. H. Smith. 2010. Mechanical breaking of microtubules in axons during dynamic stretch injury underlies delayed elasticity, microtubule disassembly, and axon degeneration. FASEB J. 24:1401–1410.

[3] Janmey, P. A., U. Euteneuer, M. Schliwa. 1991. Viscoelastic properties of vimentin compared with other filamentous biopolymer networks. J. Cell Biol. 113:155–160.

[4] Stephen J. Peter, Mohammad R. K. Mofrad, 2012, Computational Modeling of Axonal Microtubule Bundles under Tension, Biophysical Journal Vol.102 749–757

[5] Gavin A. Buxton, Sandra L. Siedlak, George Perry, Mark A. Smith, 2010, Mathematical modeling of microtubule dynamics: Insights into physiology and disease, Progress in Neurobiology92.

[6] A. Shahinnejad, M. Haghpanahi, F. Farmanzad, 2013. Finite element analysis of axonal microtubule bundle under tension and torsion, Procedia Engineering 59 16 – 24